# Accepted Manuscript

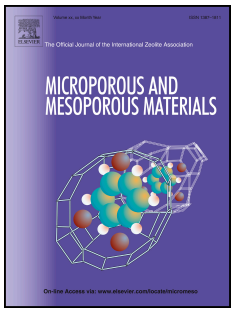


HKUST-1@ACM hybrids for adsorption applications: A systematic study of the synthesis conditions

J. Fernández-Catalá, M.E. Casco, M. Martínez-Escandell, F. Rodríguez-Reinoso, J. Silvestre-Albero

PII: S1387-1811(16)30402-4

DOI: 10.1016/j.micromeso.2016.09.020

Reference: MICMAT 7905

To appear in: *Microporous and Mesoporous Materials*

Received Date: 30 May 2016

Revised Date: 8 September 2016

Accepted Date: 13 September 2016

Please cite this article as: J. Fernández-Catalá, M.E. Casco, M. Martínez-Escandell, F. Rodríguez-Reinoso, J. Silvestre-Albero, HKUST-1@ACM hybrids for adsorption applications: A systematic study of the synthesis conditions, *Microporous and Mesoporous Materials* (2016), doi: 10.1016/j.micromeso.2016.09.020.

**Graphical Abstract**

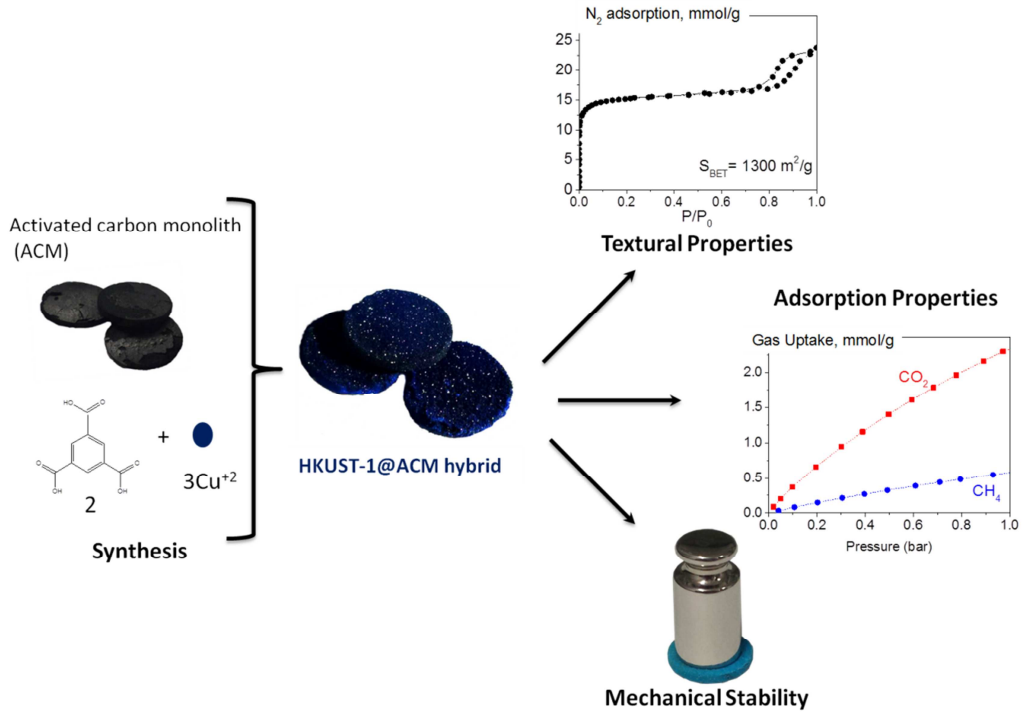

# HKUST-1@ACM hybrids for adsorption applications: A systematic study of the synthesis conditions

*J. Fernández-Catalá[a], M. E. Casco[a*], M. Martínez-Escandell[a], F. Rodríguez-Reinoso[a], J. Silvestre-Albero[a]*

[a]*Laboratorio de Materiales Avanzados, Departamento de Química Inorgánica-Instituto Universitario de Materiales, Universidad de Alicante, Ctra. San Vicente-Alicante s/n. E-03690. San Vicente del Raspeig, Spain.*

*Corresponding author. Fax: +34 965903454; Tel: +34 965909350

E-mail address: miriancasco@gmail.com

**Abstract**

This work constitutes a guide towards the preparation of metal-organic framework materials (MOF) supported and/or confined in activated carbon monoliths (ACM). The resulting hybrid porous materials exhibit improved physico-chemical properties as compared with their parent constituents. The different hybrids were obtained exploring several experimental approaches, which were thoroughly discussed. All hybrids were characterized by $N_2$ adsorption isotherms, SEM, TGA and XRD techniques. The characterization studies pointed out that the preparation conditions are of paramount importance in defining the nucleation and growth of HKUST-1, either outside of the carbon grains (surface coating), and/or in the internal pores (bulk confinement). While the surface coating was achieved by directly synthesizing the MOF in presence of the ACM (i.e. *in-situ* synthesis), bulk confinement is favored after applying an additional step that involves a pre-nucleation at low temperatures (5 °C). The hybrid material with the best performance, sample A5(1), shows enhanced mechanical properties compared to its parent counterparts, combined with high apparent surface area (up to 1300 $m^2/g$), an improved crushing strength (about 8 times superior to ACM) and a geometrical density of around 0.45 $cm^3/g$, which almost duplicates that of ACM. Last but not least, the adsorption behavior of the hybrid was tested for $CO_2$ and $CH_4$ adsorption. Application of IAST equation to the single component adsorption

isotherms at room temperature gives rise to a $CO_2/CH_4$ selectivity factor of 5.5 in the hybrid material, larger than that on ACM (S=3.5).

**Keywords:** MOF@ACM hybrids; synthesis; mechanical properties; adsorption.

## 1. Introduction

Metal-Organic Frameworks (MOFs) are a novel type of nanostructured porous material formed by metal ions or metal oxide clusters linked by organic molecules. After the activation treatment, i.e. elimination of the solvent, they show an extraordinarily large surface area and a high porosity which are tunable owing to the versatility of its chemical structure [1-2]. MOFs have attracted intensive interest in the last few years in multiple fields including storage/separation of gases [3-5], heterogeneous catalysis [6], and biomedical application such as drug delivery [7].

Among MOFs, Cu(II) benzene-1,3,5-tricarboxylate (also called HKUST-1) has shown promising results for selective $CO_2$ adsorption over $CH_4$ and $N_2$ [5]. Furthermore, it was recently published that HKUST-1 can reach the new volumetric target of the Department of Energy of the United Stated (263 V/V) for methane storage at high pressure, although these values were obtained using the crystallographic density of the MOF [3]. From a practical point of view, the consideration of the bulk density seems to be more reasonable for volumetric calculations. Unfortunately, HKUST-1 has a very low bulk density that cannot be improved using a conventional conforming step due to its delicate framework structure [8]. Our previous studies [9] have shown that growing HKUST-1 inside the cavities of a porous carbon is a promising approach to increase the mechanical properties of the MOF due to the protective role of the carbon walls against external loads, but keeping unaffected its adsorption properties. These studies have anticipated that hybrid materials are a promising alternative to overcome the conformational issues associated to MOFs.

Monoliths with both large geometrical/dimensional density and good mechanical properties are still needed instead of a fine powder in order to facilitate the material handling in the industry (e.g. eliminate dusting problems) and to achieve a reasonable working capacity in volumetric basis for gas storage or gas separation technologies (e.g. pressure swing adsorption, PSA). Herein, we propose a new method to manufacture MOF@activated carbon monolith (ACM) hybrids directly in disc-shaped

avoiding the conforming step used in previous works [8-9]. Therefore, a binderless activated carbon monolith from petroleum residue will be used as a guest structure.

Petroleum residues (ethylene tar) after the carbonization process produce a mesophase pitch (MP) that shows self-sintering ability (more details about the MP characteristics can be found elsewhere [10-11]). This property allows the mesophase grains to sinter during the activation process, allowing the preparation of nanoporous monolith without using any binder [10]. The absence of a binder anticipates that this material can be a proper clean host structure (i.e. only inert carbon in the monolith composition) to accommodate HKUST-1 nanocrystals in their cavities. In fact, the incorporation of binders, e.g. carboxymethyl cellulose or polyvinylalcohol may interact with the linker and metal salts, thus hindering the proper crystallization of the MOF. Herein we report different experimental approaches to reach an optimum nucleation and growth of the HKUST-1 using binderless activated carbon monoliths in order to prepare MOF@ACM hybrids. The main goal will be to promote the nucleation and growth of MOF not only in the exterior of the monolith (surface coating) but also in the inner cavities (preferentially macropores), that could be considered useful for any adsorption application. Adsorption properties, geometrical densities and mechanical stability of the as-synthesized hybrids will be thoroughly discussed.

## 2. Experimental

### *2.1. Synthesis of activated carbon monoliths (ACMs)*

The synthesis of the ACMs was carried out following the procedure explained in our previous work [10-11]. Briefly, a petroleum residue (ethylene tar) was carbonized in a pilot plant at 460 °C for 3 hours and at 1 bar of nitrogen. The resulting mesophase pitch (MP) was physically mixed with anhydrous KOH in a ball mill at 300 rpm for 30 minutes using KOH: MP ratio of 3:1 wt %. A disc-shaped mold with a diameter of 13 mm was filled with the required amount of the physical mixture to produce monolith of 1, 2 and 3 mm height. Taking advantage of its high plasticity, monoliths were prepared without using any binder by applying uniaxial compression of 400 MPa at room temperature. The monoliths were immediately placed into the horizontal furnace to allow the activating agent acting over the MP at 800 °C for 2 h with a heating rate of 5°C/min under inert atmosphere of 100 ml $N_2$/min. The final activated carbon

monoliths (ACMs) were carefully washed with distilled water several times up to reach pH~7, and dried in an oven overnight.

*2.2. Synthesis of HKUST-1@ACM hybrids*

Five different experimental approaches to produce hybrids were explored and studied. The knowledge gained was used to produce an optimum hybrid material whose mechanical stability and adsorption properties were evaluated.

*Approach 1:* ACMs (2 mm height) were impregnated with an oversaturated solution of the linker 1, 3, 5-tricarboxylic acid (BTC, 1 g) in ethanol (10 g) overnight in order to assure the presence of the linker in the whole carbon. Afterwards, ethanol was removed by evaporation in an oven at 85 °C and the pre-impregnated monolith (ACM@BTC) was introduced into a Teflon autoclave containing an aqueous solution of $Cu(NO_3)_2$ (0.3 g/3 ml distillated water). After 1 h at ambient temperature the autoclave was sealed and put in an oven for the hydrothermal reaction at 110 °C for 18 hours.

*Approach 2:* The synthesis followed the same procedure as in approach 1 but the drying step of the pre-impregnated monolith was avoided in order to keep ethanol in the pores.

*Approach 3:* The synthesis followed the same procedure as approach 2 but when the pre-impregnated monolith was introduced into a Teflon autoclave, 3 ml extra of ethanol were added to the Cu aqueous solution.

*Approach 4:* The synthesis followed the same procedure as approach 2 but when the pre-impregnated monolith was introduced into a Teflon autoclave, 0.1 g of BTC and 3 ml extra of ethanol were added to the Cu aqueous solution.

*Approach 5:* The synthesis followed the same procedure as approach 4, introducing an additional step which consisted in keeping the autoclave at 5 °C for 2h to favor the formation of small HKUST-1 nuclei and their migration towards the inner porosity of the carbon (ACM@nucleus). Thereafter, the autoclave was sealed and heated for the hydrothermal reaction at 110 °C for 18 hours. This approach was also tested using ACMs with a thickness varying from 1 to 3 mm. Therefore, approaches 1, 2, 3, 4 and 5 gave

rise to the hybrids called A1, A2, A3, A4, A5(1), A5(2), A5(3), the number in brackets giving the thickness of the monolith on approach 5.

*2.3. Sample characterization*

The textural characterization was measured by nitrogen adsorption isotherm at 77 K using a homemade automatic volumetric equipment now commercialized by Gas to Materials Technologies (www.g2mtech.com). Before the adsorption tests, the samples were degassed for 12 h at 150 °C. The $N_2$ adsorption data were used to determine the total pore volume ($V_t$) at a relative pressure of 0.95, the specific surface area by applying Brunauer- Emmett-Teller equation ($S_{BET}$) and the microporosity by the application of Dubinin–Radushkevich equation ($V_{N2,DR}$). The difference between $V_t$ and $V_{N2,DR}$ is considered as the mesopore volume ($V_{meso}$). Thermogravimetric analysis was carried out using a METTLER TOLEDO TGA/SDTA851e/SF/1100, under inert atmosphere (100 ml $N_2$/min) and at heating rate of 10 °C/min, unless otherwise stated. X-ray diffraction (XRD) patterns were recorded with a Bruker D8-Advance diffractometer equipped with a Goebel mirror (non-planar samples) with CuKα radiation (40 KV-40 mA). Measurements were made over a range of 5º<2θ<25º, in 0.05º step width with a 1º/min scanning rate. The bulk geometric densities were calculated using the monoliths dimension and weight. Mercury porosimetry was measured using a POREMASTER-60 GT device from Quantachrome instruments. Crushing test of the hybrids was carried out using an adaptation of the D 4179-01 ASTM standard method. Attrition test of the hybrids was carried out using a sieve shaker Mod. RP.08 (CISA) using a sieve of 800 µm in which five stainless steel balls were kept in contact with one monolith during 30 minutes at half of the maximum power. The monolith was weighted before and after the test.

*2.4. $CO_2$ and $CH_4$ adsorption*

$CO_2$ and $CH_4$ adsorption capacity at room temperature up to 1 bar were measured. Before any adsorption experiment the hybrids were degassed at 150 °C for 12 h. The analyses were performed in a home-made fully automatic volumetric equipment, now commercialized as iSorbHP by Quantachrome Instruments. A sample cell with a sectional area of 1.5 $cm^2$ was used in order to analyze the entire monolith. The Ideal Adsorption Theory (IAST) described by Myers and Prausnitz [12] was used to

calculate the selectivity factor of $CO_2$ over $CH_4$. The predicted IAST isotherms were achieved from the equation:

$$\pi_{(Pi^0)} = \frac{RT}{A}\int_{t=0}^{Pi^0} \eta i^0{}_{(t)} dlnt$$

Where $\eta i^0{}_{(t)}$ is the adsorption isotherm of the pure component i. The spreading pressure (expressed as $\frac{\pi A}{RT}$, where π is the monolayer of the gas on the surface) is calculated graphically from the area under the curve, $\eta i^0/P_i^0$ vs. $P_i^0$.

## 3. Results and discussions

The scanning electron microscopy (SEM) image (**Fig. 1 a**) of the activated carbon monolith (ACM) used as a host structure for this study, shows the presence of a single carbon skeleton matrix formed by perfectly bonded carbon particles. The void spaces, coming from the KOH particles used for the activation step and also the products of the activation process (potassium, carbonates, etc.) can be clearly identified. ACMs exhibit a well-developed macroporosity (0.8 $cm^3/g$) with a mean pore size *ca*. 0.37 μm according to Hg porosimetry results (**Fig. SI.1**). Concerning the crystal size for HKUST-1, previous studies in the literature have described crystals ranging from 200 nm to several microns depending on the synthesis variables [13]. Comparing these two values it can be anticipated that carbon macrocavities are large enough to host HKUST-1 crystals; even mesopores could allocate small HKUST-1 crystals since 2.63 nm was reported to be the unit cell dimension of this particular MOF [14]. In order to promote HKUST-1 growing in the inner cavities of the carbon, a pre-impregnation of the ACM with the linker, trimesic acid (BTC), was carried out as a first step to synthesize MOF@ACM hybrids. This strategy would favor both the initial nucleation of the MOF in the whole carbon and a better anchoring of the crystal on the carbon surface.

### *3.1. Influence of ethanol in the ACM coating*

To check the influence of ethanol in the crystal nucleation and growth of the HKUST-1, several synthesis approaches varying the amount of ethanol were performed. **Figs. 1 b-h** show the size and morphology of the crystals obtained in the interior and on the surface of the monolith (hybrids A1, A2, A3, A4).

Whereas in the approach 1 the BTC pre-impregnated monolith was directly immersed in the Cu aqueous solution, after the elimination of ethanol, in the approach 2 ethanol was kept in the pre-impregnated monolith; thereafter both syntheses followed the same procedure described in the experimental section resulting in the hybrids A1 and A2 (**Figs. 1 b-d**). Unfortunately, none of them result in the desirable HKUST-1 morphology. SEM images reveal the formation of needle-like products in both cases, far from the tridimensional porous structure of the targeted MOF. These needle-like structures are formed due to a deficient BTC coordination process, i.e. one or two of the carboxylate groups seem to be connected to the Cu center, creating a zig-zag chain, giving rise to non-porous 1-D or 2-D polymers [15, 16]. Even if larger amount of ethanol was added to the Cu aqueous solution in the approach 3, SEM images show that it was not enough to complete the coordination of the organic linker. In fact, SEM images (**Figs. 1 e and f**) show again the formation of 1-D or 2-D polymers as main product, although some crystals of HKUST-1 (hybrid A3) were formed. Whereas in hybrids A2 and A3 the interior of the monolith is homogeneously filled with the non-porous polymers structure, only in hybrid A3 the surface is partially covered with particles of HKUST-1. Taking into account these results, it is inferred that more BTC is necessary to synthesize additional crystals of HKUST-1 to completely cover the surface of the ACM.

Therefore, in the approach 4, after the pre-impregnation step, an additional solution of BTC: ethanol 1:1 %wt was added to the Cu aqueous solution. **Figs. 1 g and h** show that the resulting hybrid A4 is covered with a large amount of irregular crystals of MOF perfectly connected between them giving rise to a layer of *ca.* 100 µm thick. It also shows that this layer is penetrating the ACM, thus suggesting a good anchoring of the crystals to the carbon surface. However, additional crystals cannot be observed in the inner pores of the monolith, maybe due to the migration of the BTC from the interior of the carbon to the surface, where there is not steric hindrance for the crystal to grow.

**Fig. 2 a** illustrates the $N_2$ adsorption/desorption isotherms at 77 K of the hybrids A1, A2, A3 and A4. All the isotherms are type I(b) according to the new IUPAC classification [17] typical for microporous materials, which in principle, anticipate that these monoliths are promising materials for $CO_2$ capture. The isotherm for hybrid A4 also exhibits a small hysteresis loop in the relative pressure range 0.5-1.0, possible due to new mesopores created in the intercrystalline space of the HKUST-1 or to the interparticle space between HKUST-1 crystals and the carbon framework [13]. The nitrogen adsorption

capacity follows a clear trend A1< A2< A3< A4, which confirms that the presence of ethanol is essential to avoid the formation of the non-porous 1-D, 2-D structures and to create the desirable 3-D porous framework of HKUST-1. Table 1 shows the apparent surface areas calculated by applying the BET equation to the $N_2$ adsorption data. Considering that in A1 and A2 hybrids, only the carbon skeleton from ACM is contributing to the $N_2$ adsorption process, i.e. the second component is a non-porous polymer, the low surface areas of these hybrids (155 and 250 $m^2/g$ respectively) suggest a large blocking of the carbon porosity (original surface area of the ACM is 2000 $m^2/g$) by the undesired particles. Interestingly, the formation of crystals of HKUST-1 starts to contribute to the total surface area in the hybrid A3, increasing to 810 $m^2/g$. Finally, a much better coating is achieved in the hybrid A4 which results in an increase of the total apparent surface area to 1070 $m^2/g$.

The thermogravimetric analysis (TGA) results for the hybrid A4 are presented in **Fig. 3**. The parent materials are included for the sake of comparison**.** The TGA profile for the hybrid shows a weight loss at 100 °C that can be associated with a large amount of humidity adsorbed (*ca*. 10%), typical of hydrophilic materials such as HKUST-1. The following weight loss (~ 220 °C) can be assigned to the decomposition of the low quality crystals, but it does not reveal the weight loss corresponding to the BTC; none of the hybrids show this behavior, as it can be noted in **Fig. SI.2.** This observation suggests that the linker is participating either in the formation of the polymer or the MOF. Finally, the TG profile reveals a weight loss stage from *ca.* 300 °C to 350 °C caused by the structural decomposition of the HKUST-1 in the hybrids. Although a priori the TG profiles under the same heating rate (10ºC/min) reveal a certain improvement in the thermal stability of the confined MOF, a decrease in the heating rate to 1ºC/min (to avoid diffusional limitations of the organic molecules coming from the decomposition of the hybrid inside the carbon cavities) reveals that the confined HKUST-1 remains the thermal stability of the bulk system. Concerning the carbon host, *ca.* 20 % weight lose can be appreciated due to the release of oxygenated functional groups.

The X-ray patterns of hybrids A1 and A2 are shown in **Fig. 4**. They confirm the absence of the 3-D porous MOF when comparing with the free HKUST-1. A single peak at 10.3 °, coincident with the $Cu(BTC)(H2O)_2$ 1-D particle obtained by J. Gascón et al. [16], can be appreciated. The 1-D particle was called catena-Triaqua-μ-[1,3,5- benzenetricarboxylato (2-)]-copper(II) by Pech and Pickardt [15]. In this compounds,

only two of the three carboxylic groups of the acid act as ligands for the Cu atoms, i.e. polymeric zig-zag chains are formed rather 3D network. A mixture between the 1-D particle and the 3-D framework can be distinguished in hybrids A3 and A4 in accordance with the TGA and SEM analysis.

Summarizing, these results confirm that ethanol is of paramount importance to reach a homogeneous coating of the carbon monolith with the 3-D porous network of the HKUST-1. Although the pre-impregnation step allows the crystals to grow from the inside to the outside of the monolith, excess of BTC is required to completely cover the surface of the monolith with additional MOF. Zhang et al. proposed a possible explanation for the importance of the ethanol in the synthesis of the HKUST-1 based on the intermolecular interactions between the ethanol/water mixture and the linker. These authors suggested that the strong H-bond interaction between the water and ethanol molecules would weaken the interaction between water and BTC molecules when an amount exceeding 30 % of ethanol in a water/ethanol mixture is used. The weaker solvent-linker interaction guaranteeing that the three carboxylate groups of BTC are available to be effectively coordinated with Cu (II) [18].

*3.2. Optimization of the ACM coating/bulk confinement*

After gaining knowledge in preparing HKUST-1 crystals supported on ACM, additional effort has been carried out to improve the nucleation and growth of MOF crystals inside the inner cavities and on the surface of the ACM. For this issue, after immersing the pre-impregnated monolith on the Cu aqueous solution, the suspension was subjected to an additional quenching step at low temperature, to promote the formation of small MOF crystals. SEM images in **Fig. 5** show the different steps of this approach to obtain the hybrid A5 (1) (1 mm thickness of the original ACM). **Figs. 5 a and b** show the interior of the monolith after 1 h at room temperature and after 2 h at 5 °C, respectively. As it can be observed, the carbon surface is covered with irregular-shaped particles with morphology completely different from the 1-D, 2-D polymers, described in the previous approaches. These particles are HKUST-1 nuclei and exhibit the same degradation temperature of the hybrid A4 (see the profile of the TGA of ACM@nucleus in **Fig. SI.2**). After keeping the reactants and the ACM in contact at low temperature for 2h, the autoclave is sealed and placed into the oven to heat it up to 110 °C for 18 h to let the nucleus grow. SEM images (**Figs. 5 c and d**) reveal the formation of HKUST-1 crystals with homogeneous size of *ca.* 10 µm. It

can be also noted that the thickness of the layer formed is *ca.* 200 µm growing toward the interior of the monolith. This value duplicates the thickness of the layer in the hybrid A4. A closer look at the internal phase of the monolith shows the presence of small crystals of MOF confined in the macroporosity (**Fig. 5 d**). In other words, the incorporation of a cooling step allows the preparation of MOF@ACM hybrids where the ACM is completely covered (coating) and slightly impregnated (bulk confinement) with crystal of HKUST-1. The low temperature used limits the growth and favors the formation of a large quantity of nuclei, thus leading to the formation of small size HKUST-1 crystals that can penetrate deeper into the ACM.

**Fig. 2 b** illustrates the $N_2$ adsorption isotherms at 77 K measured throughout the different step of the approach 5. It can be noted that the impregnated ACM@BTC and the ACM@nucleus are quite coincident. This behavior reveals that the nuclei formed at this stage do not have the 3D porous structure of the HKUST-1, and consequently they do not show porosity development. Indeed, the BET surface of 400 $m^2/g$ (for ACM@nucleus) comes from the contribution of the free porosity of the ACM. On the contrary, the hybrid A5(1) exhibits an excellent development of the porosity with a specific surface area of 1300 $m^2/g$. The close knee in the isotherm at low relative pressures clearly denotes that the hybrid material exhibits a narrow microporosity. Surprisingly, it also exhibits a very remarkable hysteresis loop in the relative pressure range 0.5-1.0, possible due to new mesopores created in the intercrystalline space of the HKUST-1 [13]. The textural parameters obtained from the isotherms are summarized in **Table 1**. In comparison with the parent HKUST-1 and ACM, the hybrid A5(1) exhibits less microporosity development ($V_{N2,\ DR}$= 0.53 $cm^3/g$), although it shows a similar total pore volume ($V_{total,0.95}$= 0.70 $cm^3/g$). It is important to note that the final hybrid exhibits a density of 0.45 g /$cm^3$ that almost duplicates the density of the parent ACM, 0.27 g /$cm^3$.

In order to check the influence of the monolith thickness in the bulk nucleation/-impregnation process, ACM 1, 2 and 3 mm of thickness were used to synthesize the corresponding hybrids A5(1), A5(2) and A5(3), respectively. As it was expected, the best result in terms of porosity development (see **Fig. SI.3)** was reached using the ACM with the minimum thickness (1 mm). The differences in the BET area (Table 1) among these hybrids may be due to the different crystal imperfection of the HKUST-1 structure. X-ray diffraction patterns in **Fig. 4** confirm the presence of the HKUST-1 in hybrids A5(1), A5(2) and to a lesser

extent in A5(3). In the last sample, X-ray diffraction pattern also shows the peak corresponding to the non-porous polymer, thus explaining its low surface area.

In view of the excellent combination of density and porosity of sample A5(1), the mechanical properties of this sample were evaluated. The crushing resistance test was chosen because it gives a measure of the compressive forces that can withstand a material before collapsing, fracturing or crushing. Surprisingly, A5(1) sample showed a crushing strength of *ca.* 8 N, an eight-fold increase compared to the parent ACM (1 N). Moreover, both samples were subjected to the attrition test (see experimental section for further details). Whereas the ACM was immediately converted into powder, the same test in the hybrid material left 35 % of the material completely intact. To the best of our knowledge mechanical properties have not been reported neither for binderless activated carbon monoliths nor for MOF@ACM hybrids. Apparently, MOF nanocrystals grown in the inner carbon cavities and in the interparticle space have double function: a) acting as 3D adsorption network and b) acting as a binder unit anchoring carbon grains in close vicinity. Interestingly, this phenomenon gives rise to a large improvement in the final integrity of the resulting monolith. These results demonstrate that the MOF@ACM hybrid can be manipulated without losing their integrity and with improved mechanical properties compared to the pure carbon monoliths, which is very advantageous towards a future practical application.

### *3.3. Adsorption properties of the HKUST-1@ACM hybrids*

In order to evaluate the adsorption performance of the new hybrid materials, $CO_2$ and $CH_4$ adsorption isotherms of the parent ACM and the hybrid A5(1) were measured at room 25 °C. The adsorption isotherms up to 1 bar for the single component are shown in **Fig. 6 a.** It can be noted that in both samples the $CO_2$ adsorption capacity is much larger than that for $CH_4$, which makes the monoliths highly attractive for $CO_2$ purification from natural gas. The superior performance of the ACM is due to its larger apparent surface area (2000 $m^2/g$) and micropore volume (0.74 $cm^3/g$), as compared to the hybrid material (1300 $m^2/g$ and 0.53 $cm^3/g$). However, the scenario changes when the isotherms are expressed in volumetric basis (see **Fig. 6 b**), using the geometrical densities from Table 1. Whereas the $CO_2$ capacities at 1 bar are quite similar, *ca.* 23 and 24 V/V for the ACM and A5(1), respectively, the capacity

for $CH_4$ is still superior in the ACM (almost double) compared to the hybrid system. Therefore, the IAST (Ideal Adsorbed Solution Theory) [12] calculation method was applied to the single component isotherms to estimate the selectivity for the $CO_2/CH_4$ separation process. The selectivity factor of $CO_2$ over $CH_4$ was calculated as:

$$S_{CO_2,CH_4} = \frac{P^0_{CH_4}}{P^0_{CO_2}}$$

where $P^0_{CH_4}$ and $P^0_{CO_2}$ are the spreading pressures of each pure component obtained from the IAST predicted isotherm and they were calculated graphically as it was described elsewhere [12]. Although low, the selectivity factor for an equimolar gas mixture $CO_2/CH_4$ at 1 bar is superior in the case of the hybrid A5(1) S ~ 5.5 compared to the value (S ~3.5) for the ACM. These values are similar to those obtained by Venna et al. [19] for membranes of ZIF-8 over alumina. Moreover, in the literature were reported experimental selectivity factor values *ca.* 5.5-6.5 at 1 bar for an equimolar gas mixture $CO_2/CH_4$ for pure HKUST-1 in the powder form [20-21]. Overall, adsorption results suggest that the hybrids MOF@ACM can be a good alternative to overcome the problems associated with MOF, i.e. problems associated with a conforming step, but with clear advantages in terms of a higher $CO_2/CH_4$ selectivity and improved mechanical properties, that allow maintaining the integrity of the monolith during the routine industry handling and manipulation.

**Conclusions**

The synthesis of MOF@ACM hybrids was successfully achieved. The resulting monolith showed better performance than its parent materials for practical application. On the one side, the HKUST-1 in the hybrid is already conformed in disc-shaped without any conforming step. On the other side, the hybrid exhibited enhanced mechanical properties and a higher $CO_2/CH_4$ selectivity factor than the ACM preserving the adsorption properties of the pure HKUST-1. Currently, we are exploring others metal-organic framework supported on activated carbon in order to enhance or preserve their excellent adsorption properties but improving their mechanical stability.

**4. Appendices**

Supplementary information accompanies this paper.

**5. Acknowledgements**

This work was supported by MINECO projects: MAT2013-45008-p. MEC wants to thank the Spanish Government for the fellowship FPU AP2010-4920.

**6. Reference**

[1] O. Farha, I. Eryazici, N. Jeong, B. Hauser, C. Wilmer, A. Sarjeant, R. Snurr, S. Nguyen, A. Yazaydın and J. Hupp, J. Am. Chem. Soc. 134 (2012) 15016.

[2] F. Hiroyasu, K. Nakeun, G. Yong, A. Naoki, C. Sang, C. Ewoo, Y. Özgür, R. Snurr, M. O'Keeffe, K. Jaheon, O. Yaghi, Science 329 (2010) 424.

[3] Y. Peng, V. Krungleviciute, I. Eryazici, J. Hupp. O. Farha and T. Yildirim, J. Am. Chem. Soc. 135 (2013) 11887.

[4] J. Liu, P. Thallapally, B. McGrail, D. Brown and J. Liu, Chem. Soc. Rev. 41 (2012) 2308.

[5] K. Sumida, D. Rogow, J. Mason, T. McDonald, E. Bloch, Z. Herm, T. Bae and Jeffrey R. Long, Chem Rev. 112 (2012) 724.

[6] A. Corma, H. García and F. Xamena, Chem. Rev. 110 (2010) 4606.

[7] C. Wang, D. Liu and W. Lin, J. Am. Chem. Soc. 135 (2013) 13222.

[8] M.E. Casco, M. Martínez-Escandell, E. Gadea-Ramos, K. Kaneko, J. Silvestre-Albero, F. Rodríguez-Reinoso, Chem. Mat. 27 (2015) 959

[9] M.E Casco, J. Fernández-Catalá, M. Martínez-Escandell, F. Rodríguez-Reinoso, E.V. Ramos-Fernández, J. Silvestre-Albero, Chem. Commun. 81 (2015) 14191.

[10] J.M. Ramos-Fernández, M. Martínez-Escandell, F. Rodríguez-Reinoso, Carbon 46 (2008) 384.

[11] A. Silvestre-Albero, J.M. Ramos-Fernández, M. Martínez-Escandell, A. Sepúlveda-Escribano, J. Silvestre-Albero, F. Rodríguez-Reinoso, Carbon 48 (2010) 548.

[12] A.L. Myers, J.M. Prausnitz. AIChE J. 11 (1965) 121.

[13] l.H. Wee, M.R. Lohe, N. Janssens, S. Kaskel, J.A. Martens. J. Mater. Chem. 22 (2012) 13742.

[14] S.S.Y. Chui, S.M.F. Lo, J.P.H. Charmant, A.G. Orpen, I.D. Williams. Science 283 (1999) 1148.

[15] R. Pech, J. Pickardt. Acta cryst. C44 (1988) 992.

[16] J. Gascón, S. Aguado and F. Kapteijn, Microp. Mesopor. Mat. 113 (2008) 132.

[17] M. Thommes, K. Kaneko, A.V. Neimark, J.P. Olivier, F. Rodríguez-Reinoso, J. Rouquerol, K.S.W. Sing, Pure Appl. Chem. 87 (9-10) (2015) 1051.

[18] B. Zhang, J. Zhan, C. Liu, X. Sang, L. Peng, X. Ma, T. Wu, B. Han, G. Yang, RSC Adv. 5 (2015) 37691.

[19] S.R. Venna, M.A. Carreon, J. Am. Chem. Soc. 132 (2010) 76.

[20] L. Hamon, E. Jolimaître, G. Pirngruber, Ind. Eng.Chem. Res. 49 (2010) 7497.

[21] J.M. Simmons, H. Wu, W. Zhouab, T. Yildirim, Energy Environ. Sci. 4 (2011) 2177.

**TABLES CAPTIONS**

**Table 1.** Textural properties of hybrid materials. ACM and HKUST-1 are included for the sake of comparison.

**FIGURE CAPTIONS**

**Fig. 1.** SEM images comparing different synthesis: (a) original ACM; (b) profile of the hybrid A1; (c), (e) and (g) surface of the hybrids A2, A3 and A4, respectively; (d), (f) and (h) interior of the hybrids A2, A3 and A4, respectively.

**Fig. 2.** $N_2$ adsorption isotherm at 77 K for the hybrids (a) A1, A2, A3, A4; (b) A5(1), HKUST-1, ACM, the pre-impregnated ACM@BTC and ACM@nucleus.

**Fig. 3.** TG analysis for the A4 hybrid material, ACM and HKUST-1.

**Fig. 4.** XRD patterns of all of the hybrids materials and powder HKUST-1.

**Fig. 5.** SEM images from different synthesis steps of A5 (1): (a) nucleus after impregnation at room temperature, (b) nucleus after cooling at 5 °C; (c) HKUST-1 crystal on the carbon surface; (d) interior of the A5(1).

**Fig. 6.** $CO_2$ and $CH_4$ adsorption isotherms for the samples ACM and A5(1) expressed in (a) gravimetric basis, (b) volumetric basis.

| Sample | $S_{BET}$ ($m^2/g$) | $V_{N2,DR}$ ($cm^3/g$) | $V_{total,0.95}$ ($cm^3/g$) | $V_{meso}$ ($cm^3/g$) | Density* ($g/cm^3$) | MOF** % |
|---|---|---|---|---|---|---|
| **HKUST-1** | 1760 | 0.65 | 0.72 | 0.07 | - | 100 |
| **ACM** | 2000 | 0.74 | 0.83 | 0.09 | 0.27 | 0 |
| **A1** | 155 | 0.07 | 0.09 | 0.02 | 0.46 | 29 |
| **A2** | 250 | 0.11 | 0.12 | 0.01 | 0.50 | 45 |
| **A3** | 810 | 0.32 | 0.35 | 0.03 | 0.44 | 43 |
| **A4** | 1070 | 0.42 | 0.47 | 0.05 | 0.48 | 61 |
| **A5(1)** | 1300 | 0.53 | 0.70 | 0.13 | 0.45 | 70 |
| **A5(2)** | 870 | 0.36 | 0.47 | 0.11 | 0.47 | 62 |
| **A5(3)** | 600 | 0.25 | 0.30 | 0.05 | 0.48 | 57 |
| **ACM@BTC** | 470 | 0.20 | 0.21 | 0.01 | 0.38 | 8 |
| **ACM@nucleus** | 430 | 0.18 | 0.19 | 0.01 | 0.39 | 33 |

*Geometric density

** Calculated by weigh

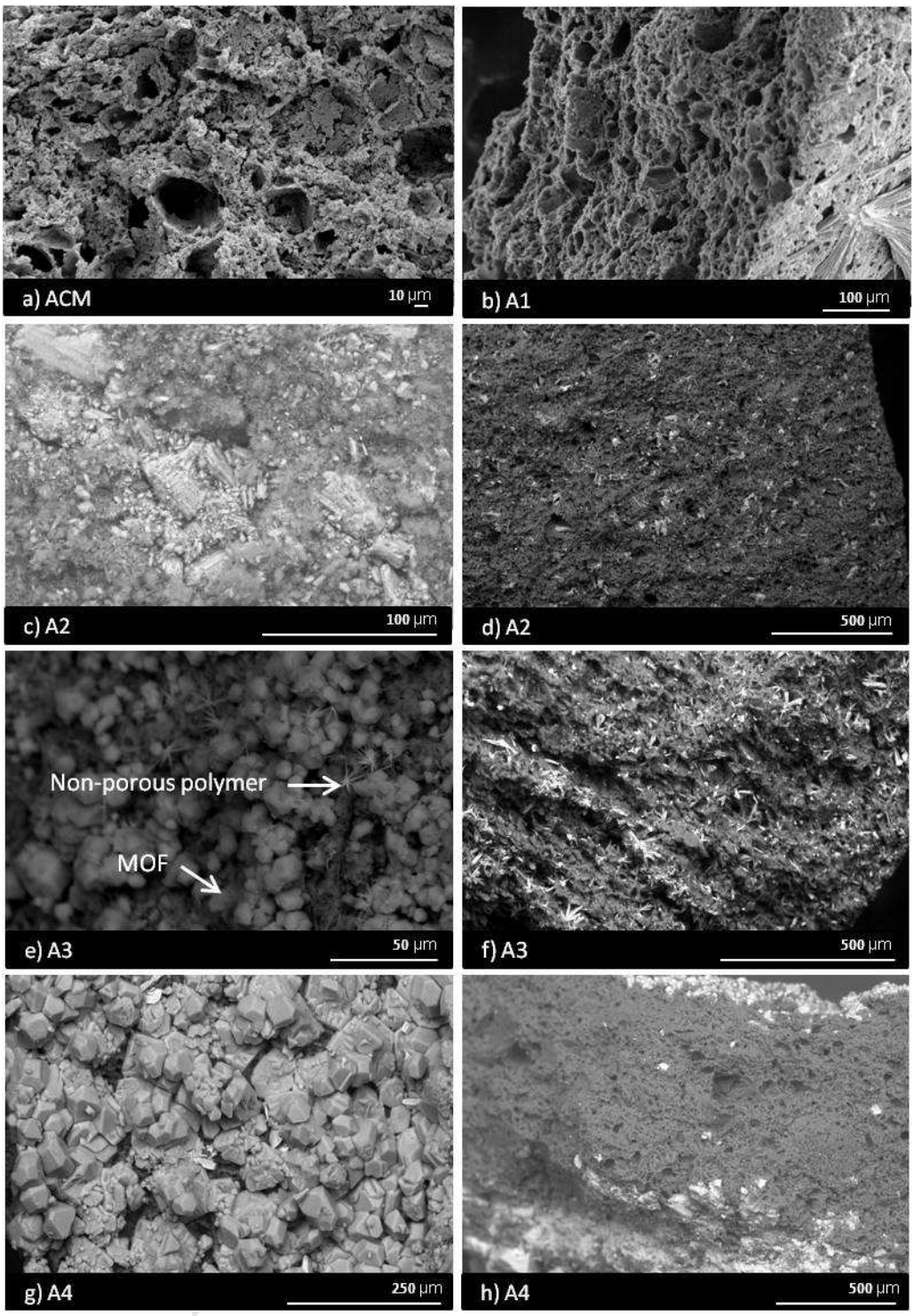
a) ACM
10 µm
b) A1
100 µm
c) A2
100 µm
d) A2
500 µm
Non-porous polymer
MOF
e) A3
50 µm
f) A3
500 µm
g) A4
250 µm
h) A4
500 µm

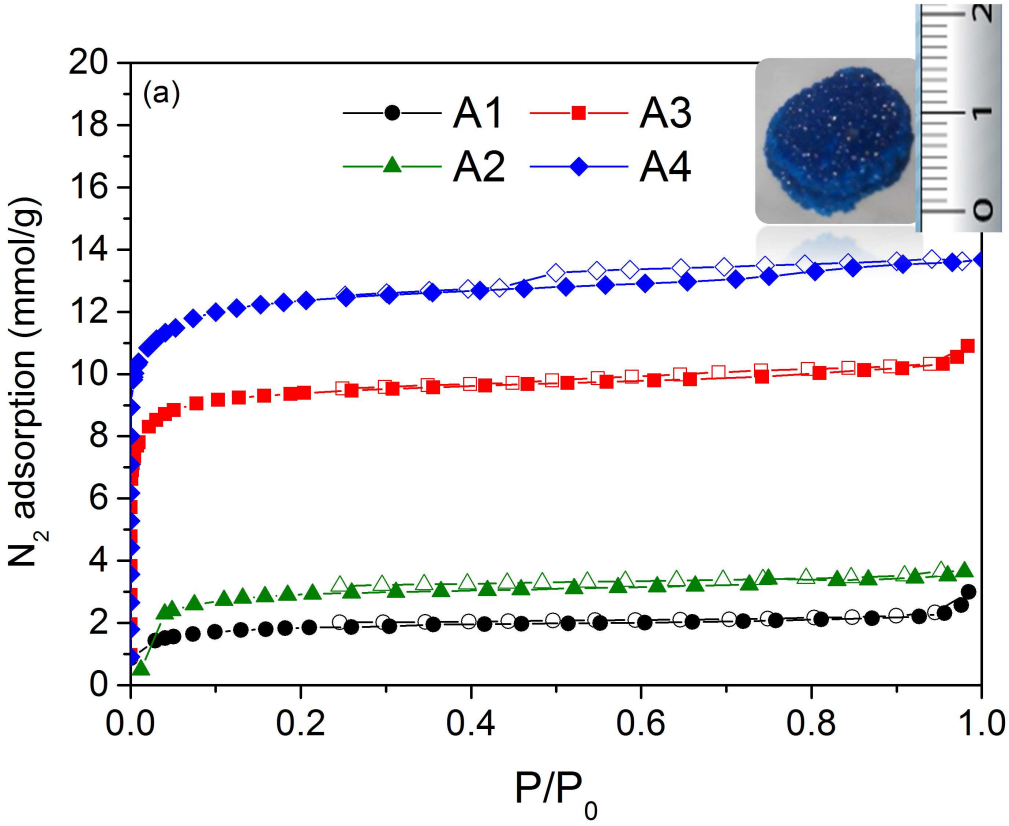

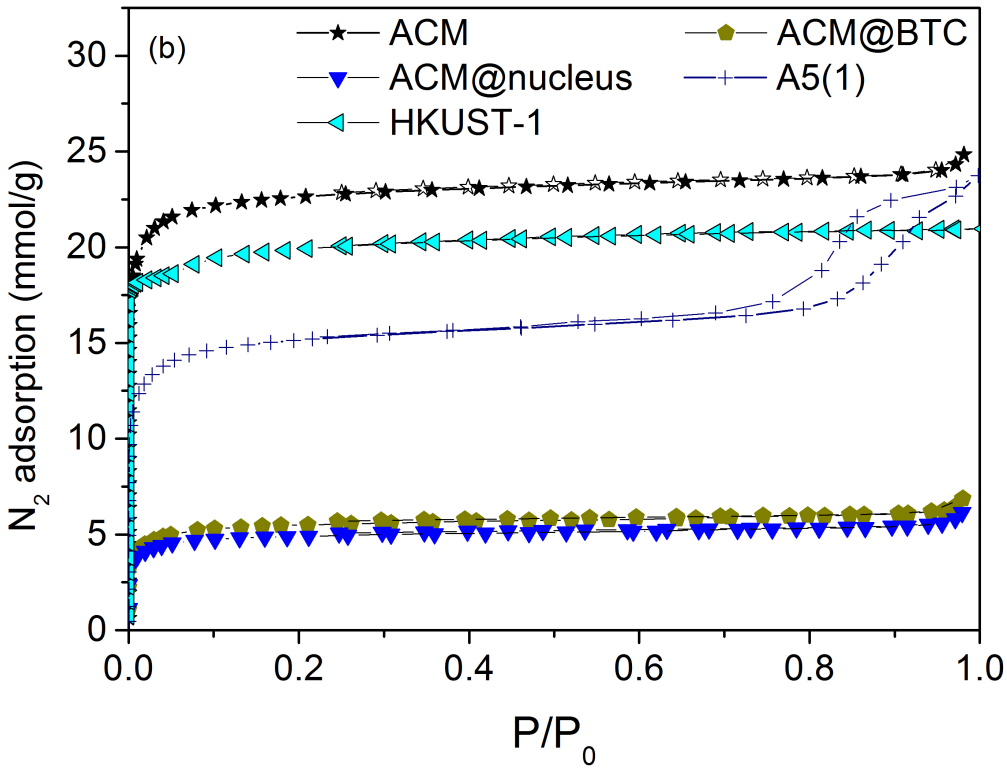

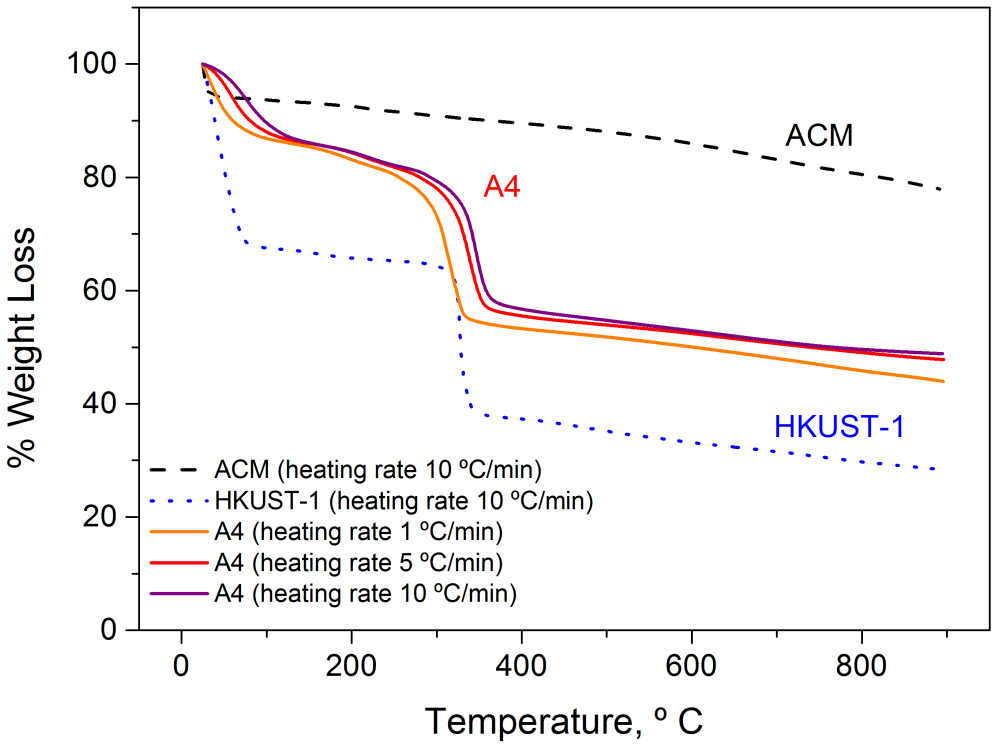
100
80
60
40
20
0
% Weight Loss
0
200
400
600
800
Temperature, º C
ACM
A4
HKUST-1
ACM (heating rate 10 ºC/min)
HKUST-1 (heating rate 10 ºC/min)
A4 (heating rate 1 ºC/min)
A4 (heating rate 5 ºC/min)
A4 (heating rate 10 ºC/min)

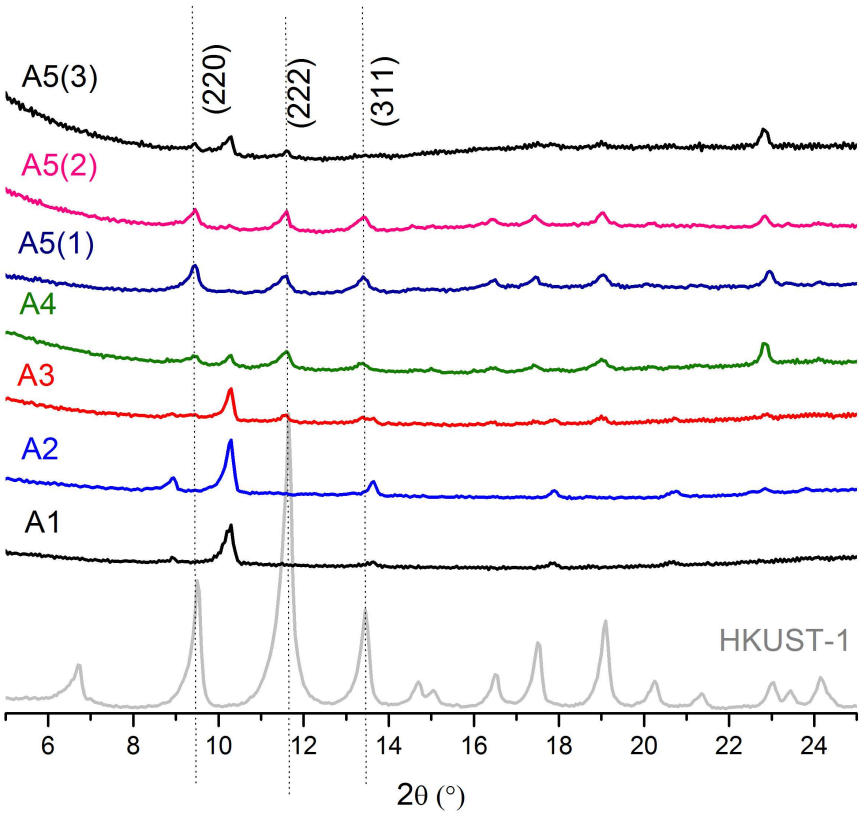

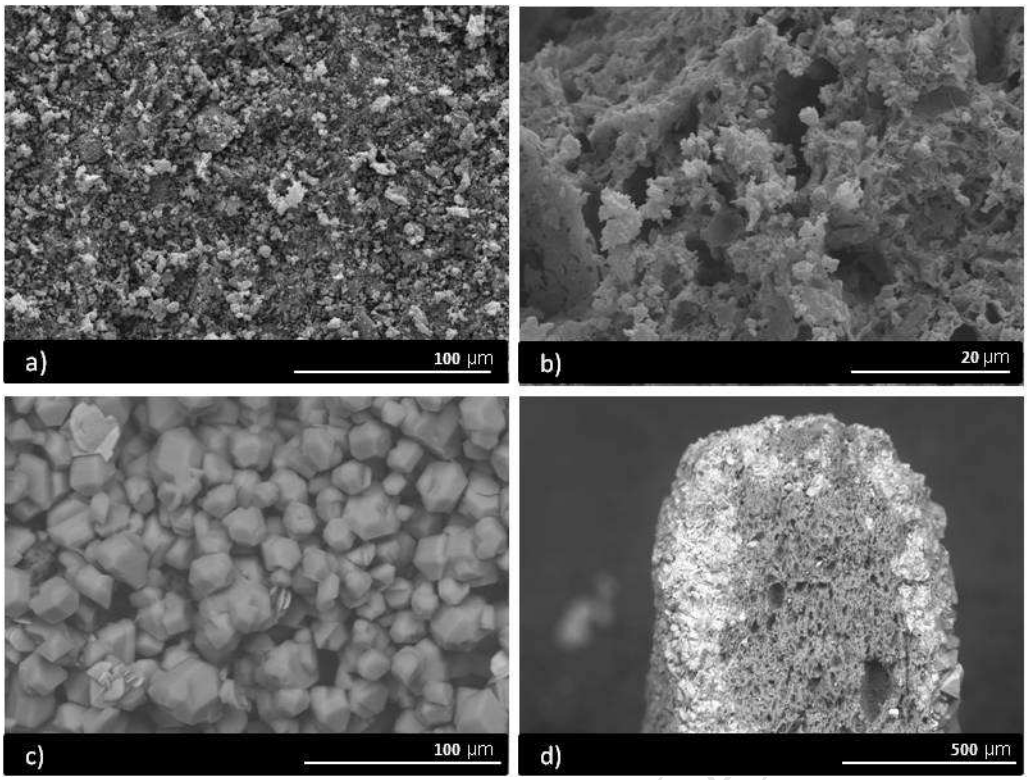

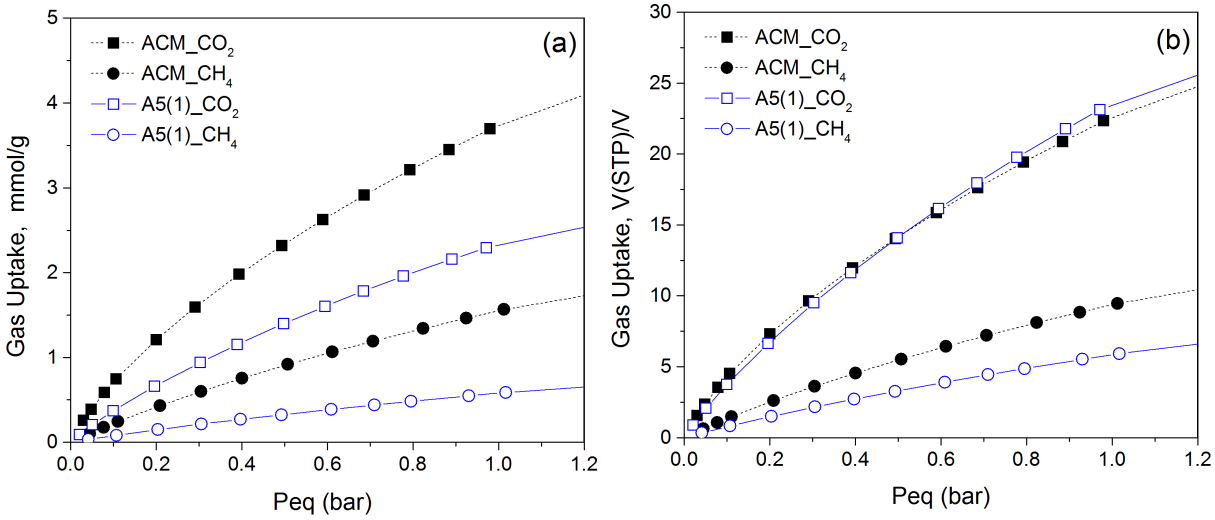

Highlights

- Preparation of HKUST-1 supported and/or confined in ACM is proposed and studied.
- HKUST-1@ACM hybrid monolith showed enhanced mechanical properties than the ACM.
- HKUST-1@ACM hybrid showed higher CO2/CH4 selectivity factor than the ACM.